SUPPORTING INFORMATION

4-Methyl/phenyl-1,2,5,6-tetraazafluoranthen-3(2*H*)-ones Synthesis: Mechanistic Pathway Study and Single-Crystal X-ray Analysis of the Intermediates

Ahmed A. M. Sarhan [1], Matti Haukka [2], Assem Barakat [3,*], Saied M. Soliman [4], Ahmed T. A. Boraei [5,*], Manar Sopaih [5] and Eid E. Salama [5]

[1] Chemistry Department, Faculty of Science, Arish University, Al-Arish 45511, Egypt; ahmed_sarhan252@yahoo.com

[2] Department of Chemistry, University of Jyväskylä, P.O. Box 35, FI-40014 Jyväskylä, Finland; matti.o.haukka@jyu.fi

[3] Department of Chemistry, College of Science, King Saud University, P.O. Box 2455, Riyadh 11451, Saudi Arabia

[4] Chemistry Department, Faculty of Science, Alexandria University, P.O. Box 426, Alexandria 21321, Egypt; saeed.soliman@alexu.edu.eg

[5] Chemistry Department, Faculty of Science, Suez Canal University, Ismailia 41522, Egypt; manar_shalabi@science.edu.eg (M.S.); eidsalama2000@gmail.com or eid_mohamed@science.suez.edu.eg (E.E.S.);

* Correspondence: ambarakat@ksu.edu.sa (A.B.); ahmed_tawfeek83@yahoo.com or ahmed_boraei@science.suez.edu.eg (A.T.A.B.); Tel.: +966-11467-5901 (A.B.); Fax: +966-11467-5992 (A.B.)

NMR Spectra

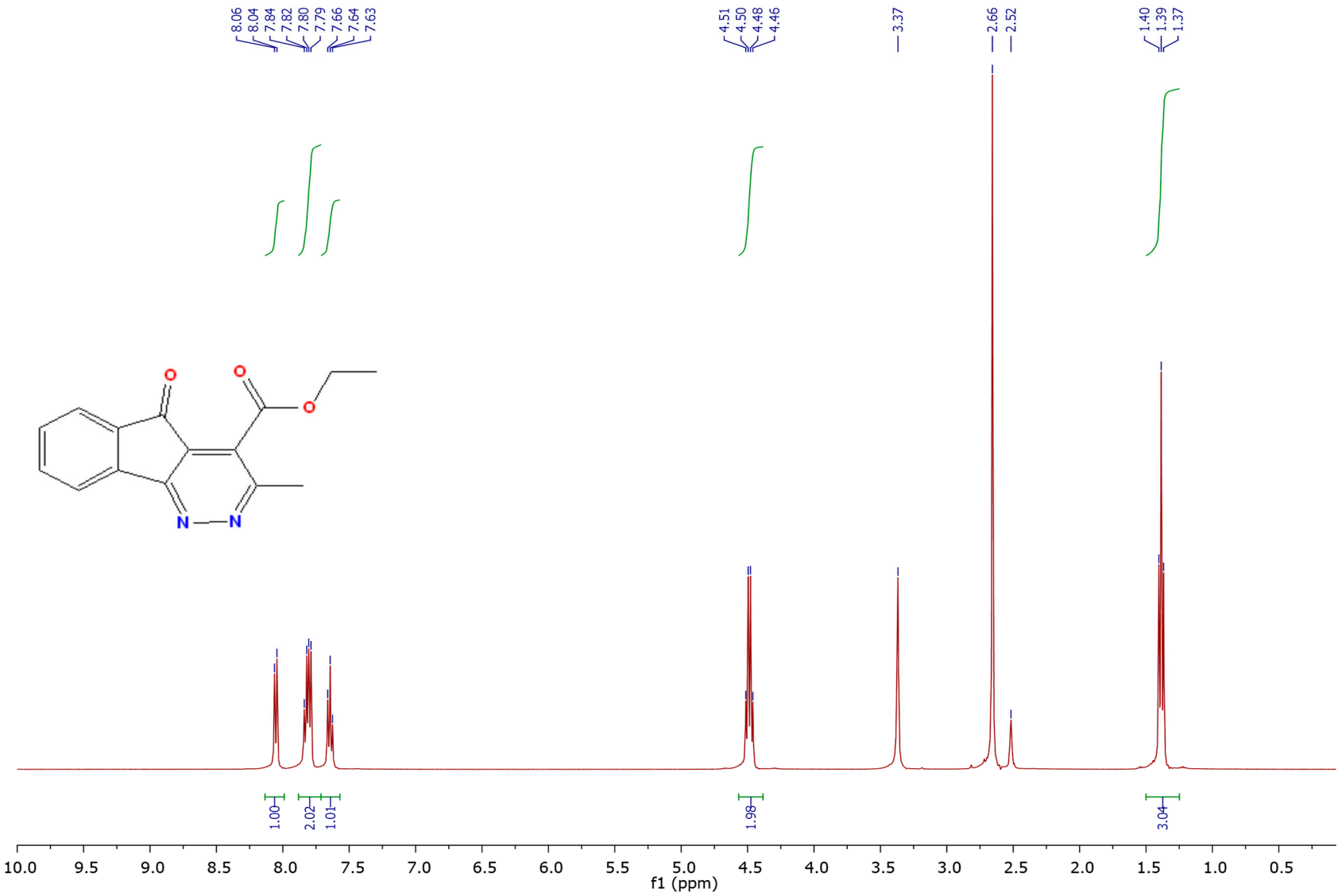

Figure S1. ^{1}H NMR of **8**

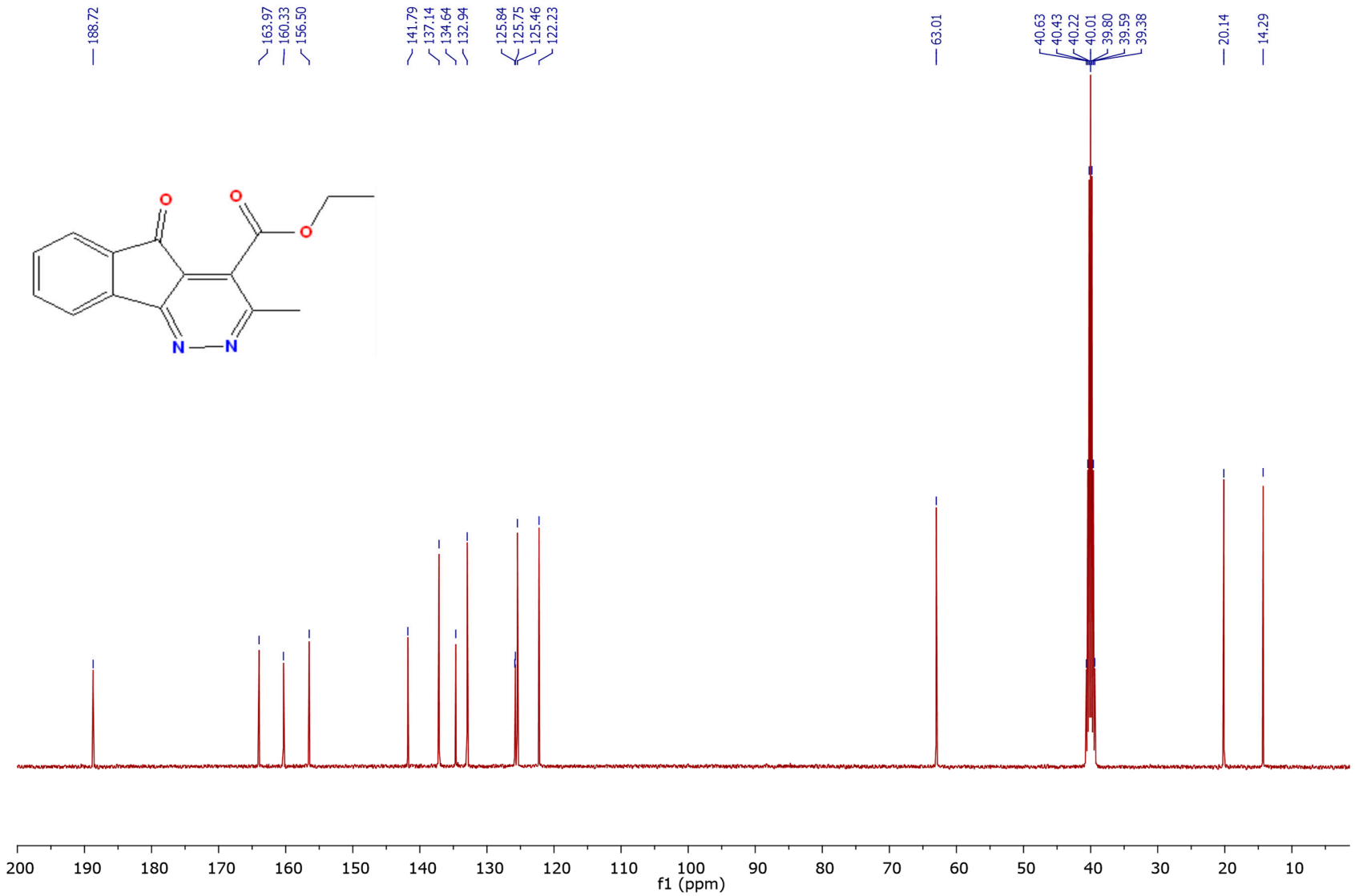

Figure S2. ^{13}C NMR of **8**

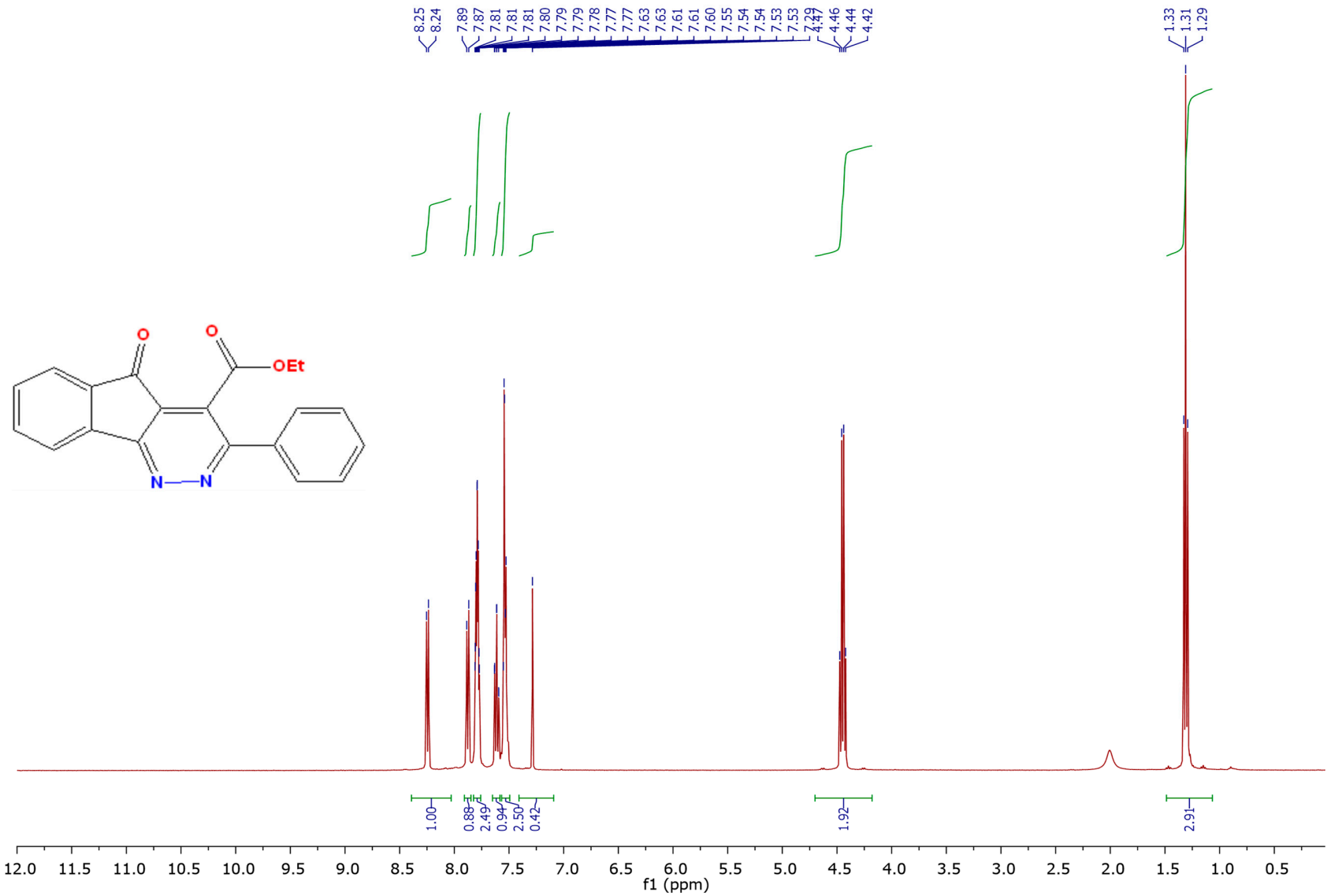

Figure S3. ^{1}H NMR of **10**

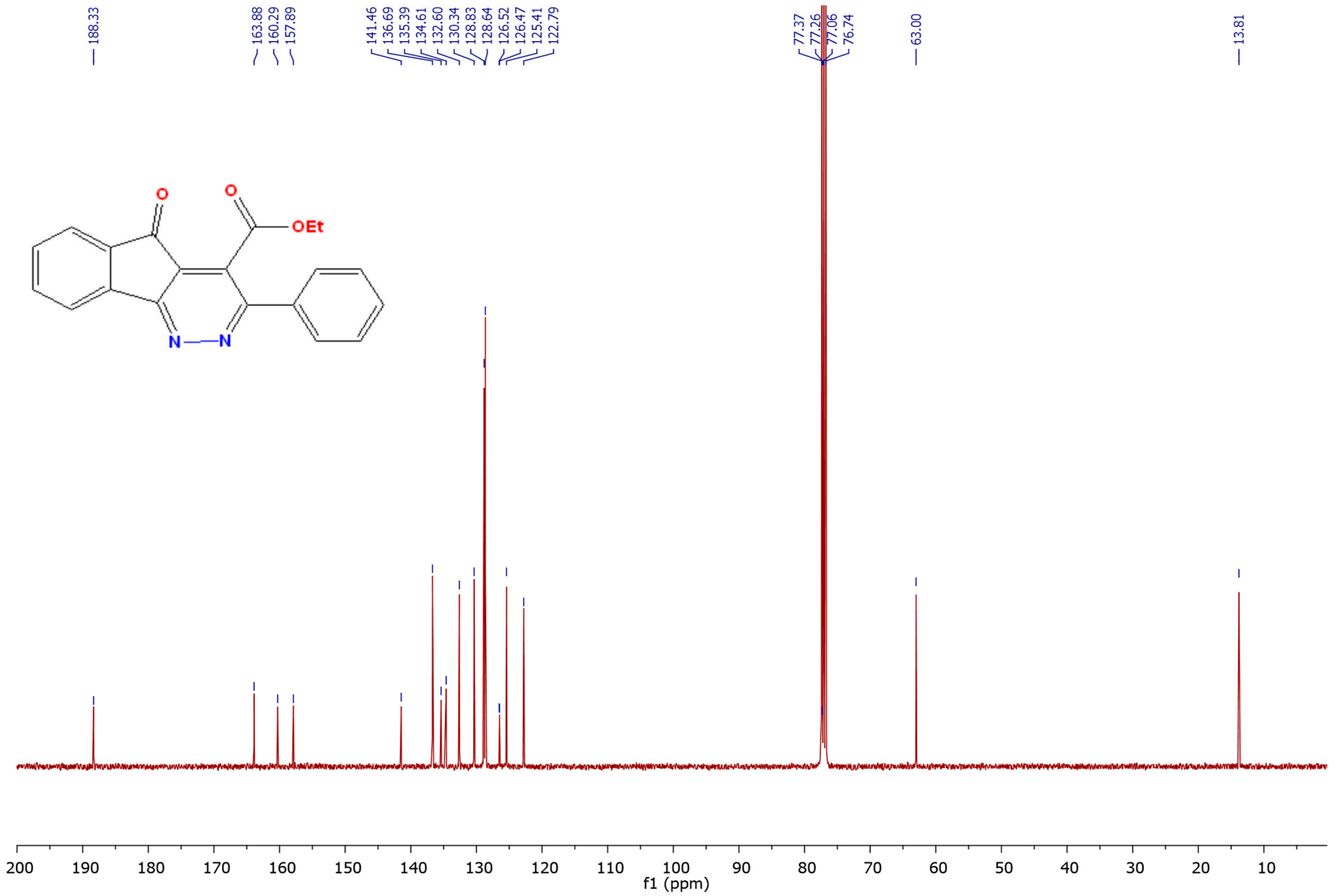

Figure S4. ^{13}C NMR of **10**

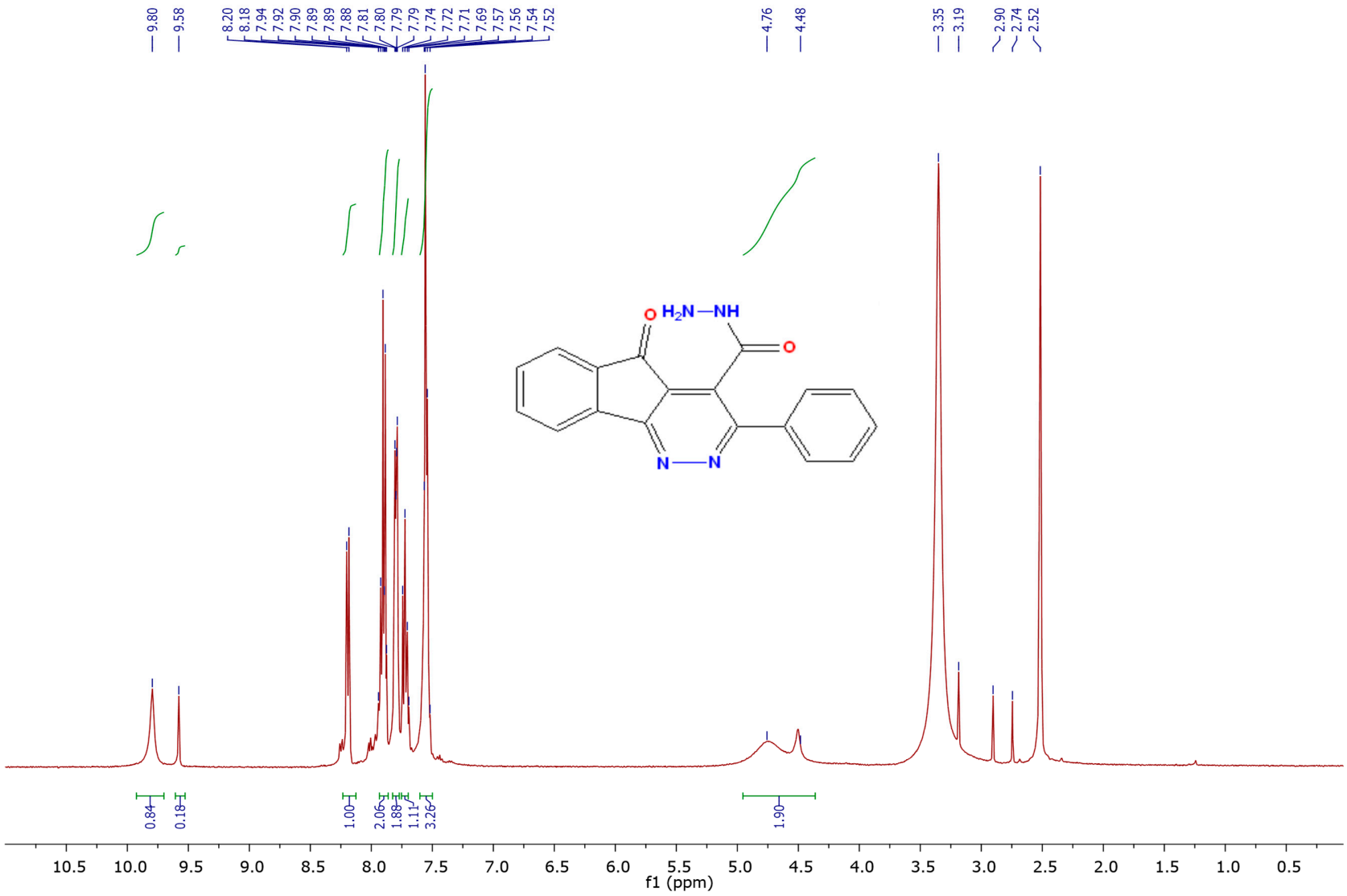

Figure S5. ^{1}H NMR of **11**

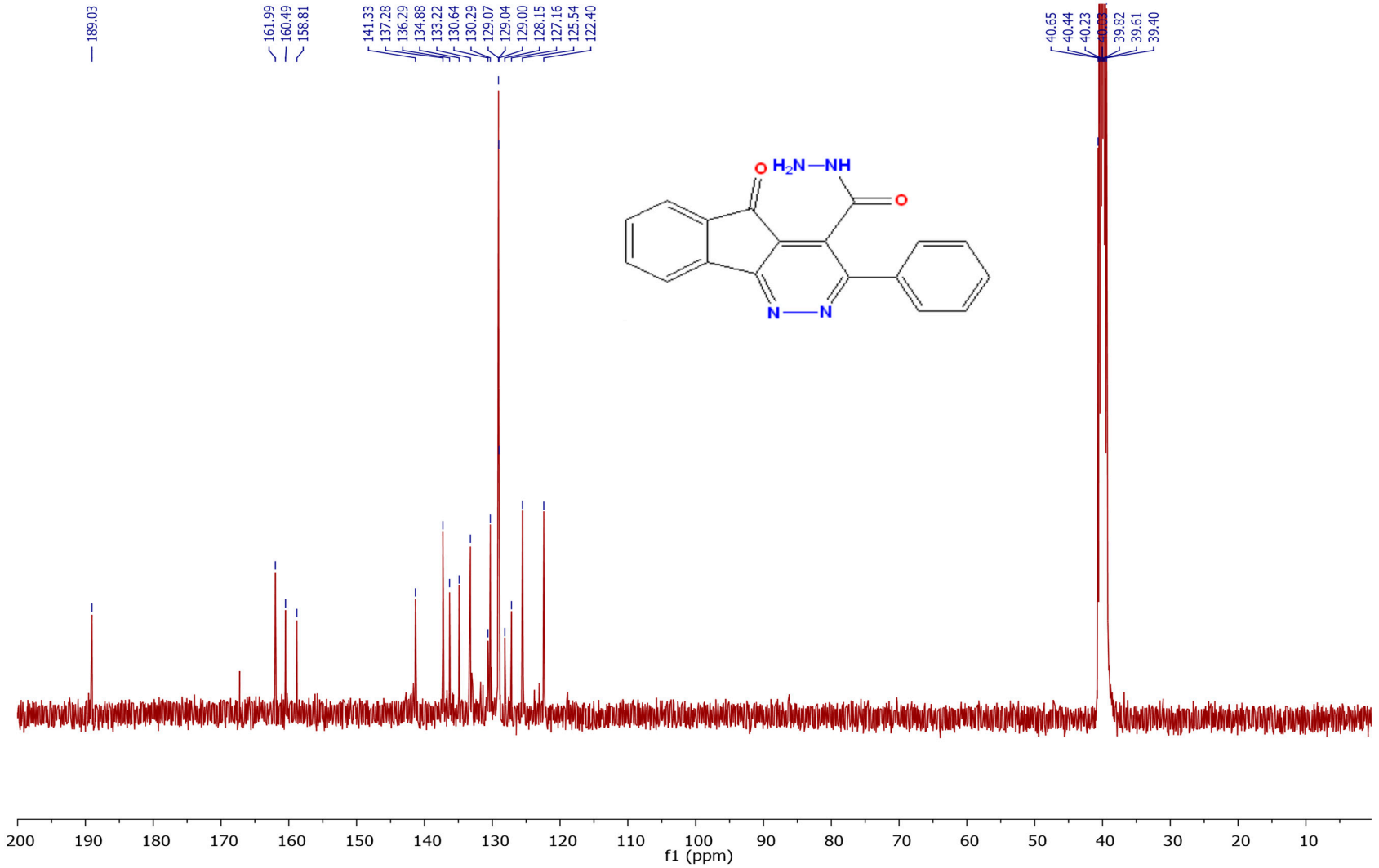

Figure S6. ^{13}C NMR of **11**

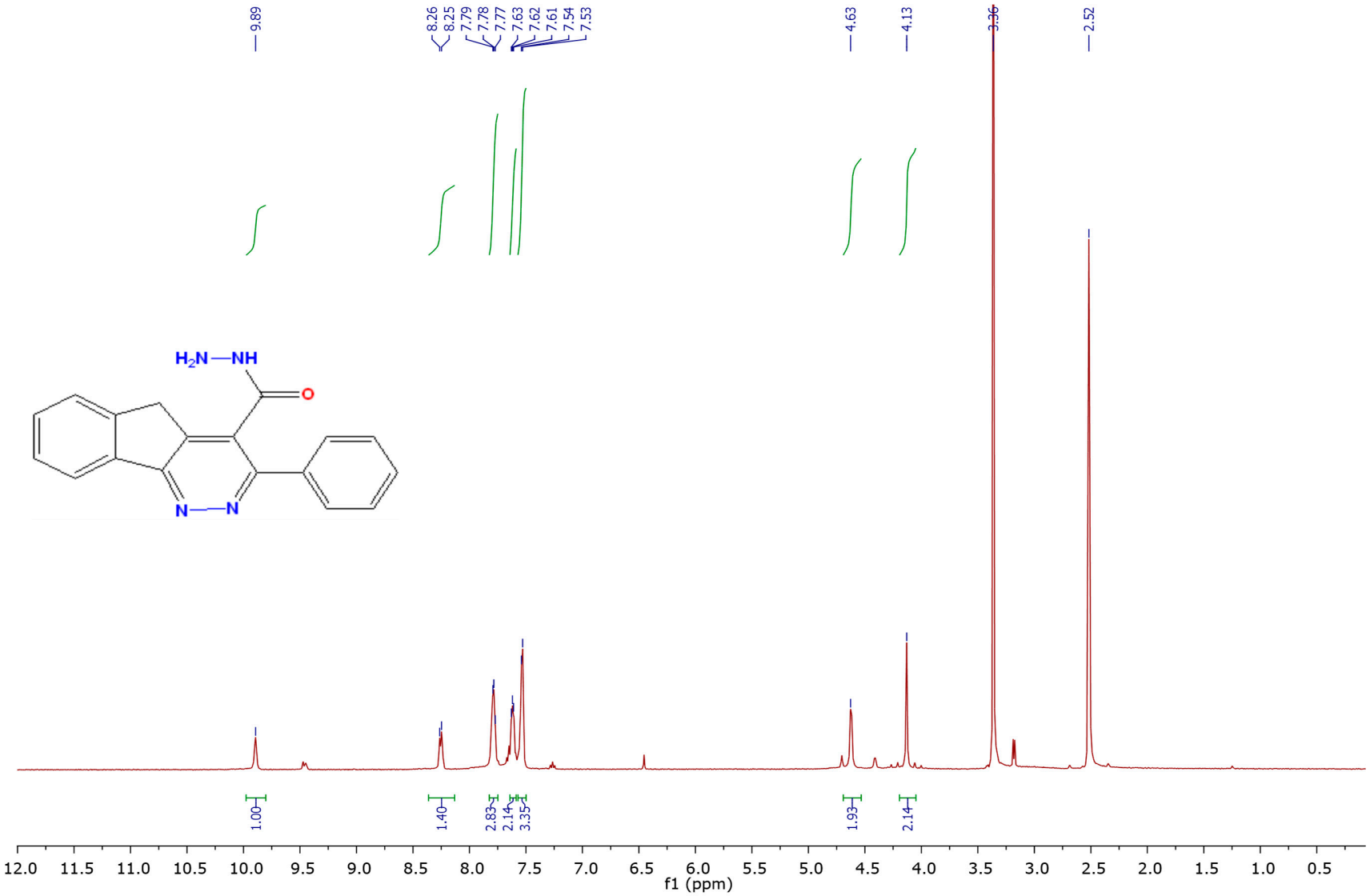

Figure S7. ^{1}H NMR of **12**

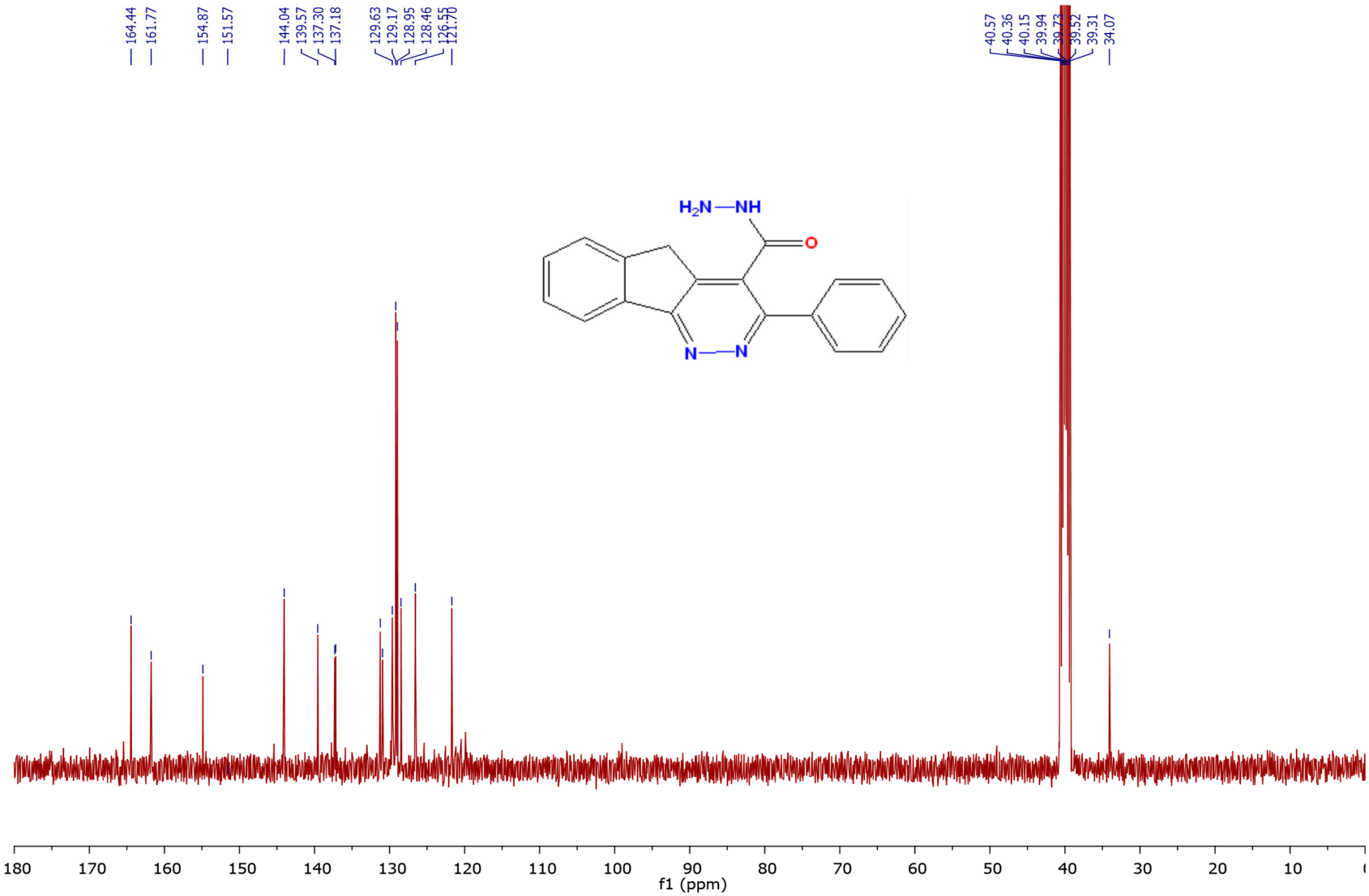

Figure S8. ^{13}C NMR of **12**

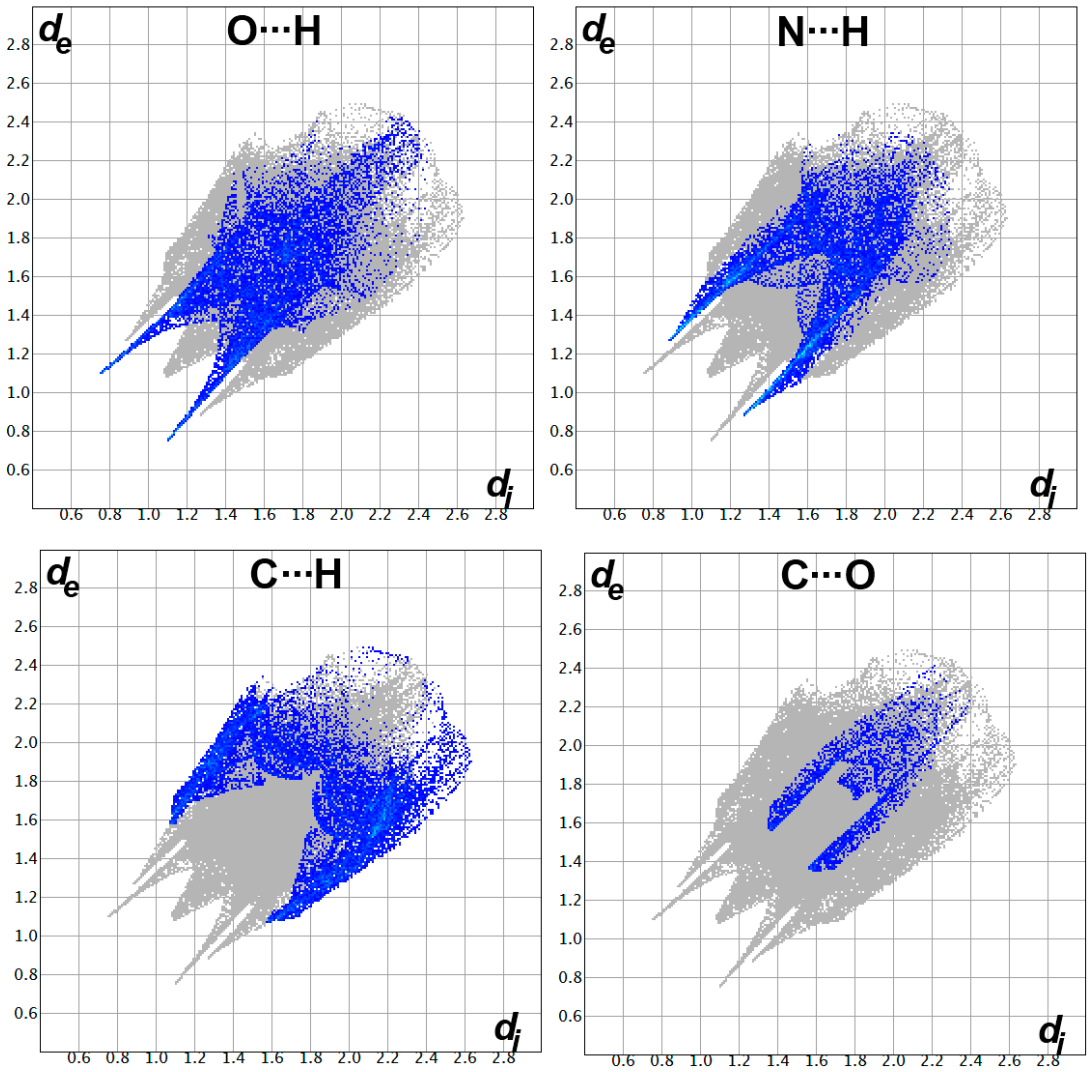

Figure S9. Fingerprint plots for the short interactions in **11**.

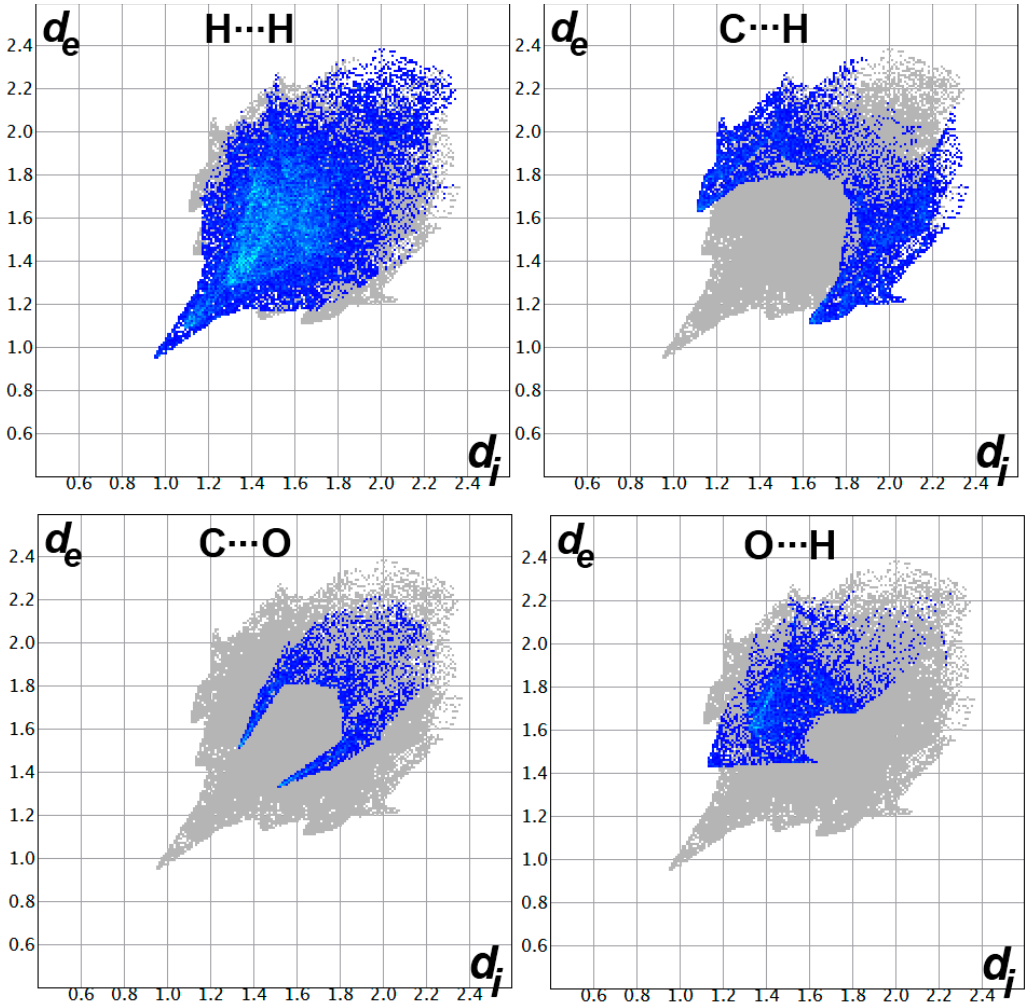

Figure S10. Fingerprint plots for the short interactions in **8**.

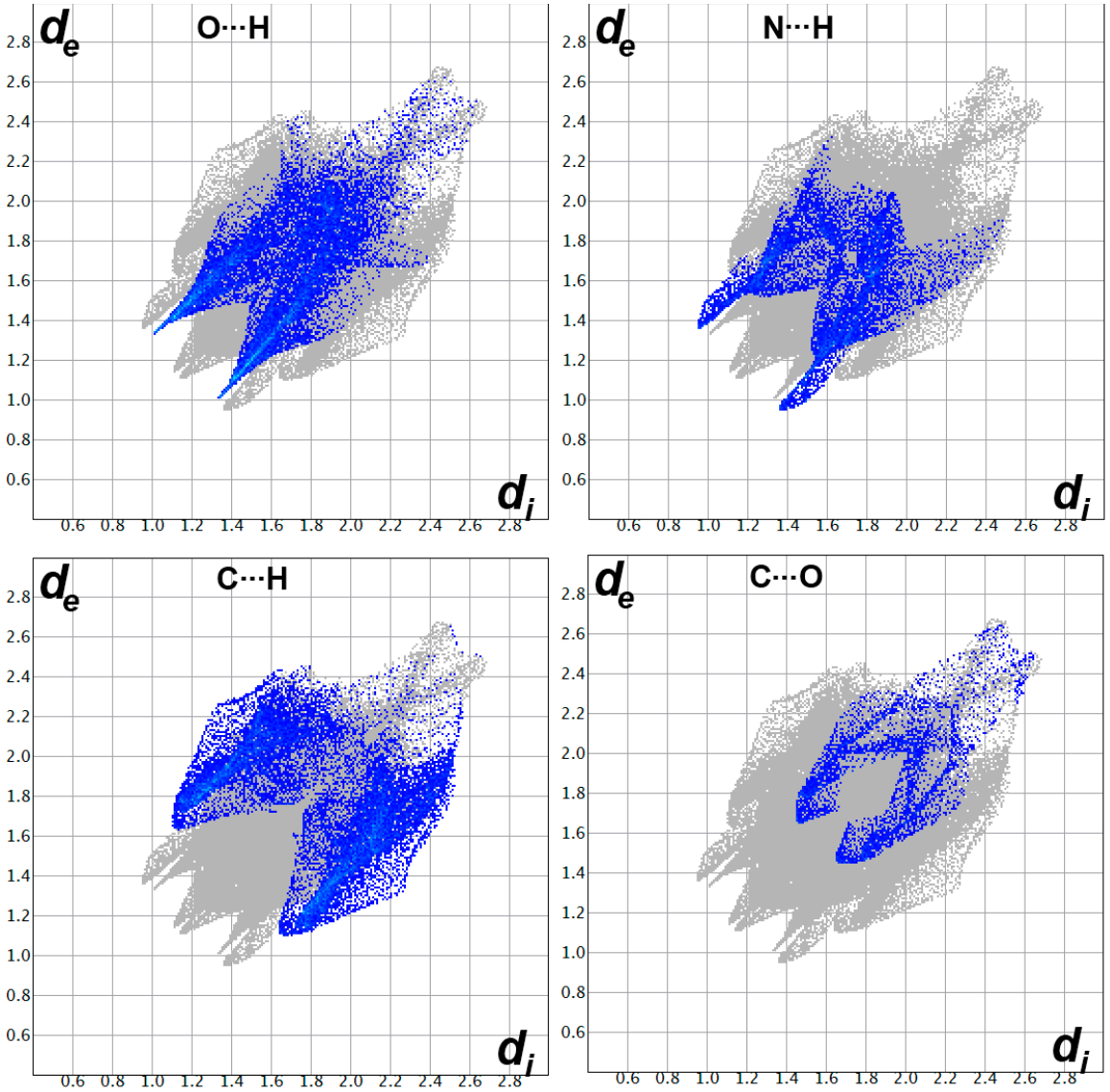

Figure S11. Fingerprint plots for the short contacts in **9**.

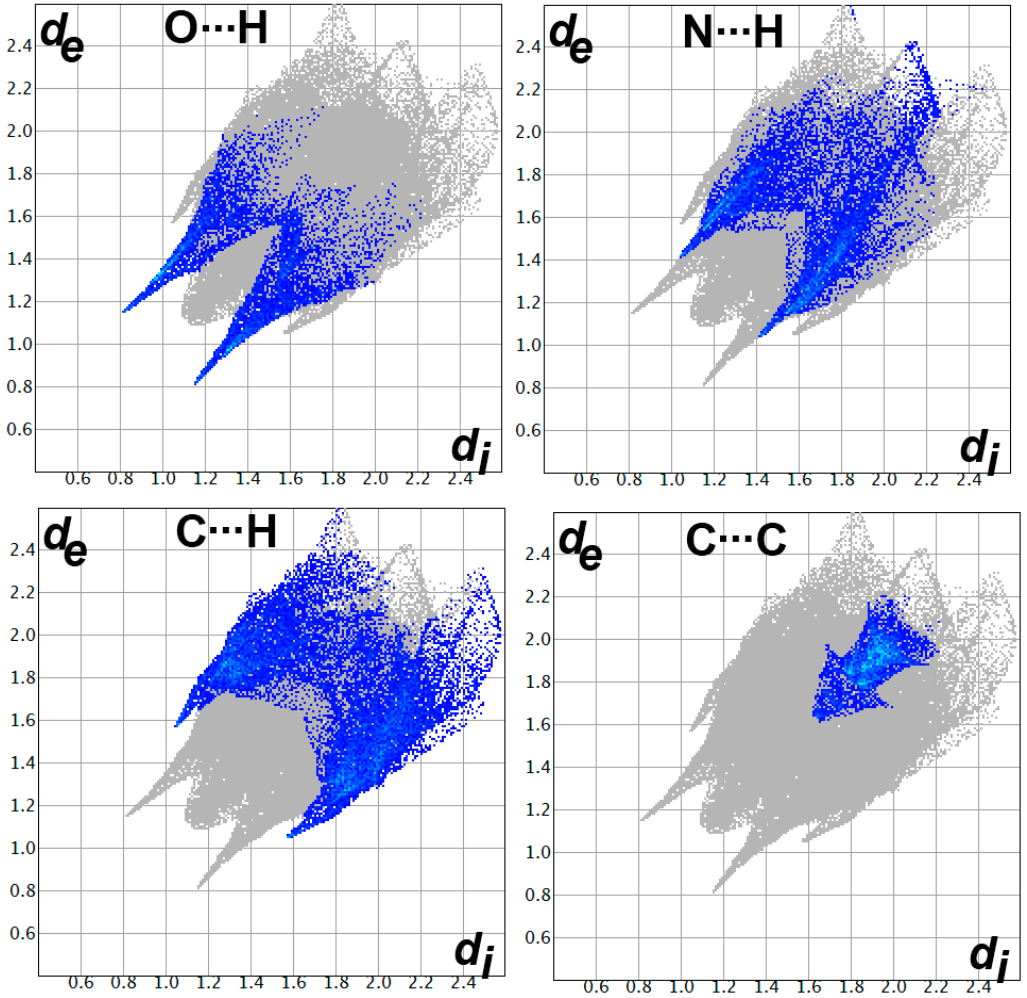

Figure S12. Fingerprint plots for the short contacts in **12**.

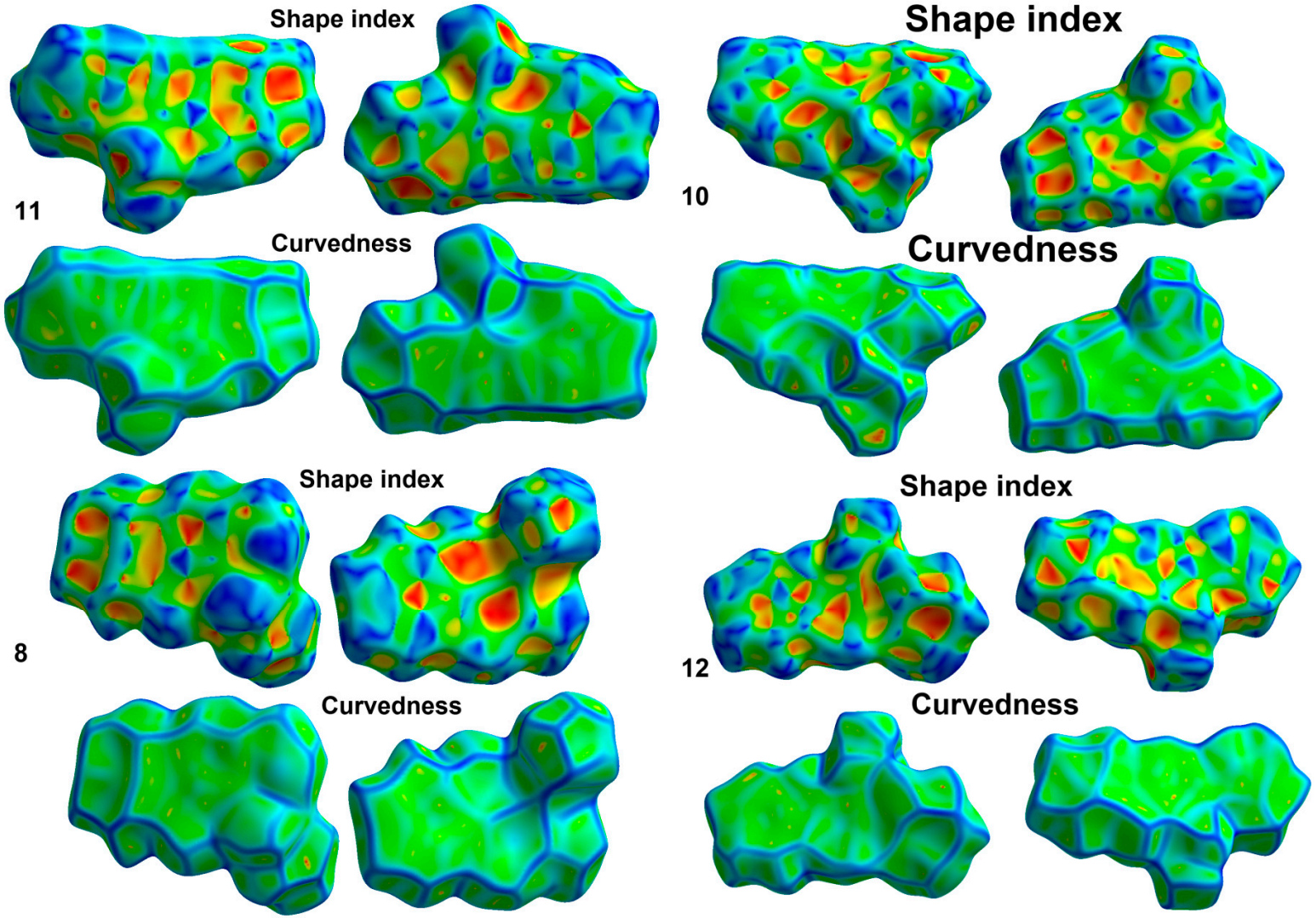

Figure S13. Shape index and curvedness maps for the studied systems.

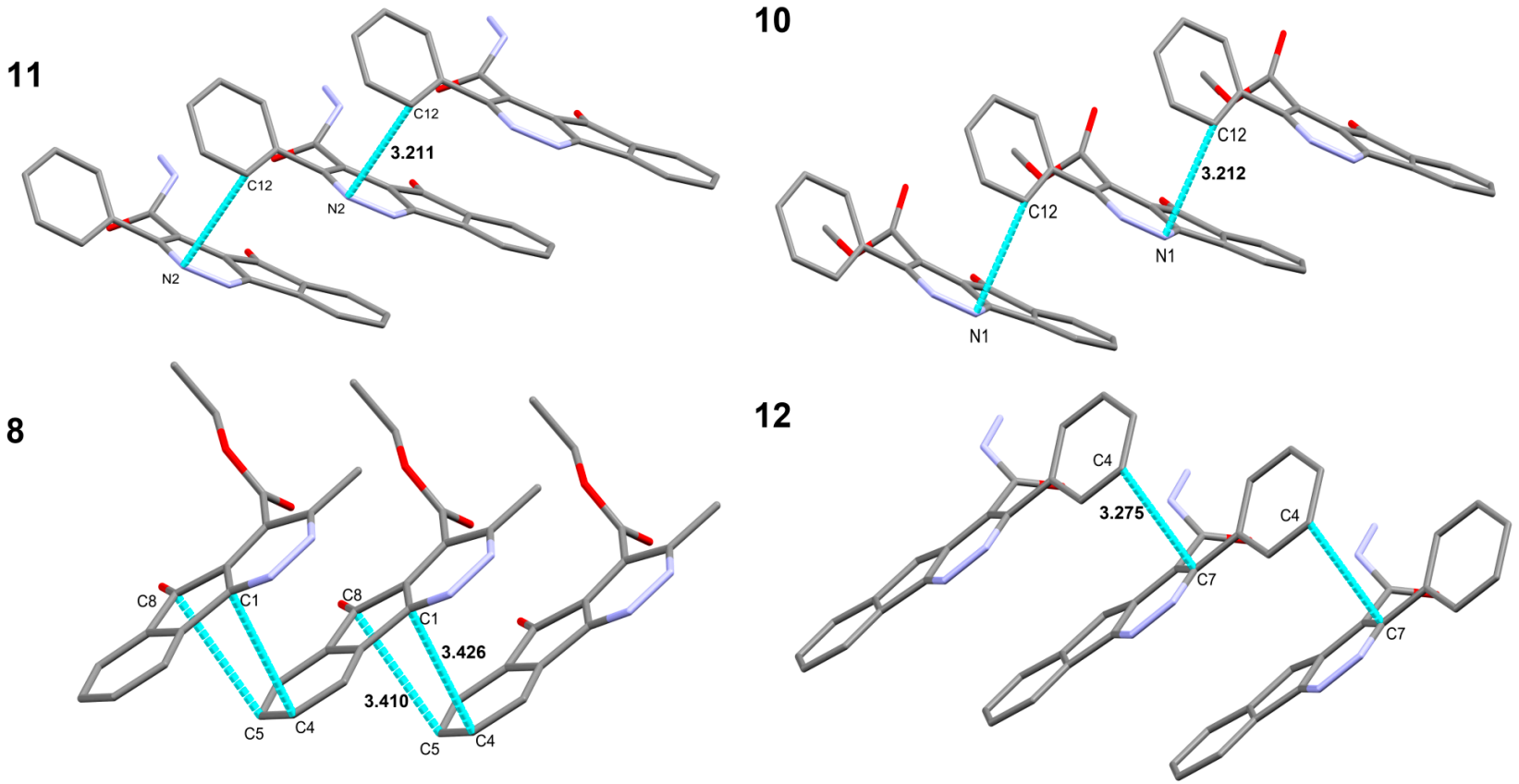

Figure S14. The most important π-π stacking C…C/C…N contacts and their interaction distances in Å for the studied systems.

X-Ray structure determination

Crystals **8**, **10, 11** and **12** were immersed in cryo-oil, mounted in a loop, and measured at a temperature of 120 K. The X-ray diffraction data were collected on a Rigaku Oxford Diffraction Supernova diffractometer using Cu Kα radiation. The *CrysAlisPro* [34] software package was used for cell refinement and data reduction. A multi-scan **9** and **11** or a Gaussian **8** and **12** absorption correction (*CrysAlisPro*) [35] was applied to the intensities before the structure solution. The structures were solved by the intrinsic phasing (*SHELXT*) [36] method. Structural refinements were carried out using *SHELXL* [36] software with *SHELXLE* [37] graphical user interface. The structure of **8** was found to be a two-component twin (twin matrix [1.000 0.000 0.333 0.000 -1.000 0.000 0.000 0.000 -1.000]). The BASF value was refined to 0.45. The NH and NH_2 hydrogen atoms in **11**, and **12** were located from the difference Fourier map and refined isotropically. All other hydrogen atoms were positioned geometrically and constrained to ride on their parent atoms, with C-H = 0.95-0.99 Å and U_{iso} = 1.2-1.5·U_{eq}(parent atom). The crystallographic details are summarized in Table 1. The topology analyses were performed using Crystal Explorer 17.5 program [38].

Table S1. Bond lengths (Å) and angles (°) for **11**, **8, 10** and **12**.

11		**8**		**10**		**12**	
Bond length (Å)							
O(1)-C(2)	1.2059(17)	O(1)-C(8)	1.2132(15)	O(1)-C(7)	1.2126(13)	O(11)-C(9)	1.240(2)
O(2)-C(18)	1.2234(18)	O(2)-C(11)	1.1974(16)	O(2)-C(18)	1.2050(13)	N(11)-C(9)	1.335(3)
N(1)-C(9)	1.3194(18)	O(3)-C(11)	1.3260(15)	O(3)-C(18)	1.3275(13)	N(11)-N(12)	1.420(2)
N(1)-N(2)	1.3542(17)	O(3)-C(12)	1.4595(15)	O(3)-C(19)	1.4684(13)	N(13)-C(18)	1.325(3)
N(2)-C(10)	1.3391(18)	N(1)-C(1)	1.3206(16)	N(1)-C(9)	1.3207(14)	N(13)-N(14)	1.345(3)
N(3)-C(18)	1.3401(18)	N(1)-N(2)	1.3603(17)	N(1)-N(2)	1.3525(13)	N(14)-C(7)	1.343(3)
N(3)-N(4)	1.4142(16)	N(2)-C(14)	1.3350(19)	N(2)-C(10)	1.3396(14)	O(11)-C(9)	1.240(2)
Bond angle (°)							
C(9)-N(1)-N(2)	117.43(11)	N(2)-C(14)-C(15)	116.20(12)	C(18)-O(3)-C(19)	115.06(8)	C(9)-N(11)-N(12)	121.75(18)
C(10)-N(2)-N(1)	121.35(11)	O(2)-C(11)-O(3)	125.89(12)	C(9)-N(1)-N(2)	117.31(9)	C(7)-N(14)-N(13)	121.36(19)
C(18)-N(3)-N(4)	121.23(12)	O(2)-C(11)-C(10)	124.69(11)	C(10)-N(2)-N(1)	121.36(9)	C(2)-C(1)-C(6)	120.2(2)
O(1)-C(2)-C(3)	127.32(13)	O(3)-C(11)-C(10)	109.41(10)	C(6)-C(1)-C(2)	117.88(11)	C(3)-C(2)-C(1)	120.6(2)
O(1)-C(2)-C(1)	128.13(13)	O(3)-C(12)-C(13)	106.53(11)	N(1)-C(9)-C(8)	124.34(10)	C(4)-C(3)-C(2)	119.5(2)
O(2)-C(18)-N(3)	124.94(13)	C(11)-O(3)-C(12)	116.58(10)	N(1)-C(9)-C(5)	126.62(9)	C(5)-C(4)-C(3)	120.2(2)
O(2)-C(18)-C(17)	121.51(12)	C(1)-N(1)-N(2)	116.95(11)	C(8)-C(9)-C(5)	109.04(9)	O(11)-C(9)-N(11)	122.25(18)
N(1)-C(9)-C(1)	124.29(13)	C(14)-N(2)-N(1)	121.51(11)	N(2)-C(10)-C(17)	122.54(10)	O(11)-C(9)-C(8)	122.98(19)
N(1)-C(9)-C(8)	126.29(12)	N(1)-C(1)-C(9)	124.44(12)	N(2)-C(10)-C(11)	115.00(9)	N(11)-C(9)-C(8)	114.74(18)
C(1)-C(9)-C(8)	109.42(11)	N(1)-C(1)-C(2)	126.82(12)	O(2)-C(18)-O(3)	125.90(10)	C(1)-C(6)-C(7)	122.71(19)
N(2)-C(10)-C(17)	122.46(12)	N(2)-C(14)-C(10)	122.52(12)	O(2)-C(18)-C(17)	121.58(10)	N(14)-C(7)-C(8)	122.56(19)
N(2)-C(10)-C(11)	114.04(11)	N(2)-C(14)-C(15)	116.20(12)	O(3)-C(18)-C(17)	112.52(9)	N(14)-C(7)-C(6)	113.24(18)
N(3)-C(18)-C(17)	113.54(12)	O(2)-C(11)-O(3)	125.89(12)	O(3)-C(19)-C(20)	109.56(10)	C(8)-C(7)-C(6)	124.19(19)